Research Article Vol. 7, No. 12 | 1 Dec 2016 | BIOMEDICAL OPTICS EXPRESS 5182

Biomedical Optics EXPRESS

Classification and analysis of human ovarian tissue using full field optical coherence tomography

SREYANKAR NANDY,[1] MELINDA SANDERS,[2] AND QUING ZHU[1,*]

[1]*Department of Biomedical Engineering, Washington University in St. Louis, USA*
[2]*University of Connecticut Health Center, Division of Pathology, USA*
[*]*zhu.q@wustl.edu*

Abstract: In this study, a full field optical coherence tomography (FFOCT) system was used to analyze and classify normal and malignant human ovarian tissue. 14 ovarian tissue samples (7 normal, 7 malignant) were imaged with the FFOCT system and five features were extracted by analyzing the normalized image histogram from 56 FFOCT images, based on the differences in the morphology of the normal and malignant tissue samples. A generalized linear model (GLM) classifier was trained using 36 images, and sensitivity of 95.3% and specificity of 91.1% was obtained. 20 images were used to test the model, and a sensitivity of 91.6% and specificity of 87.7% was obtained.

OCIS codes: (110.4500) Optical coherence tomography; (170.6935) Tissue characterization; (170.3890) Medical optics instrumentation; (170.4440) ObGyn; (170.1610) Clinical applications.

References and links

1. American Cancer Society, "Cancer Facts & Figures", American Cancer Society, Atlanta, Ga, USA, (2012).
2. T. R. Rebbeck, H. T. Lynch, S. L. Neuhausen, S. A. Narod, L. Van't Veer, J. E. Garber, G. Evans, C. Isaacs, M. B. Daly, E. Matloff, O. I. Olopade, and B. L. Weber; Prevention and Observation of Surgical End Points Study Group, "Prophylactic oophorectomy in carriers of BRCA1 or BRCA2 mutations," N. Engl. J. Med. **346**(21), 1616–1622 (2002).
3. W. A. Rocca, B. R. Grossardt, M. de Andrade, G. D. Malkasian, and L. J. Melton 3rd, "Survival patterns after oophorectomy in premenopausal women: a population-based cohort study," Lancet Oncol. **7**(10), 821–828 (2006).
4. A. Aguirre, Y. Ardeshirpour, M. M. Sanders, M. Brewer, and Q. Zhu, "Potential role of coregistered photoacoustic and ultrasound imaging in ovarian cancer detection and characterization," Transl. Oncol. **4**(1), 29–37 (2011).
5. T. Wang, Y. Yang, U. Alqasemi, P. D. Kumavor, X. Wang, M. Sanders, M. Brewer, and Q. Zhu, "Characterization of ovarian tissue based on quantitative analysis of photoacoustic microscopy images," Biomed. Opt. Express **4**(12), 2763–2768 (2013).
6. A. A. Tanbakuchi, J. A. Udovich, A. R. Rouse, K. D. Hatch, and A. F. Gmitro, "In vivo imaging of ovarian tissue using a novel confocal microlaparoscope," Am. J. Obstet. Gynecol. **202**(1), 90 (2010).
7. Y. Yang, T. Wang, N. C. Biswal, X. Wang, M. Sanders, M. Brewer, and Q. Zhu, "Optical scattering coefficient estimated by optical coherence tomography correlates with collagen content in ovarian tissue," J. Biomed. Opt. **16**(9), 090504 (2011).
8. S. Nandy, H. S. Salehi, T. Wang, X. Wang, M. Sanders, A. Kueck, M. Brewer, and Q. Zhu, "Correlating optical coherence elastography based strain measurements with collagen content of the human ovarian tissue," Biomed. Opt. Express **6**(10), 3806–3811 (2015).
9. L. P. Hariri, G. T. Bonnema, K. Schmidt, A. M. Winkler, V. Korde, K. D. Hatch, J. R. Davis, M. A. Brewer, and J. K. Barton, "Laparoscopic optical coherence tomography imaging of human ovarian cancer," Gynecol. Oncol. **114**(2), 188–194 (2009).
10. A. Dubois, L. Vabre, A. C. Boccara, and E. Beaurepaire, "High-resolution full-field optical coherence tomography with a Linnik microscope," Appl. Opt. **41**(4), 805–812 (2002).
11. A. Dubois and A. C. Boccara, "Full-field optical coherence tomography" in Optical Coherence Tomography, E.D. W. Drexler and J. G. Fujimoto, eds. (Springer, 2009), pp. 565–591.
12. A. D. Aguirre, J. Sawinski, S.-W. Huang, C. Zhou, W. Denk, and J. G. Fujimoto, "High speed optical coherence microscopy with autofocus adjustment and a miniaturized endoscopic imaging probe," Opt. Express **18**(5), 4222–4239 (2010).
13. O. Assayag, M. Antoine, B. S. Zafrani, M. Riben, F. Harms, A. Burcheri., K. Grieve, E. Dalimier, B. L. C. de Poly,and C. Boccara, "Large Field, High Resolution Full-Field Optical Coherence Tomography: A Preclinical Study of Human Breast Tissue and Cancer Assessment," Technol. Cancer Res. Treat. **13**(5), 455–468 (2014).

#275468 http://dx.doi.org/10.1364/BOE.7.005182
Journal © 2016 Received 7 Sep 2016; revised 9 Nov 2016; accepted 9 Nov 2016; published 17 Nov 2016

Biomedical Optics EXPRESS

14. M. Jain, N. Narula, B. Salamoon, M. M. Shevchuk, A. Aggarwal, N. Altorki, B. Stiles, C. Boccara, and S. Mukherjee, "Full-field optical coherence tomography for the analysis of fresh unstained human lobectomy specimens," J. Pathol. Inform. **4**(26), 26 (2013).
15. E. Dalimier and D. Salomon, "Full-Field Optical Coherence Tomography: a New Technology for 3D High-Resolution Skin Imaging," Dermatology (Basel) **224**(1), 84–92 (2012).
16. I.T. Peters, P.L. Stegehuis, R. Peek, F.L. Boer, E.W. van Zwet, J. Eggermont, J.R. Westphal, P.J. Kuppen, J.B. Trimbos, C.G. Hilders, B.P. Lelieveldt, C.J. van de Velde, T. Bosse, J. Dijkstra, A.L. Vahrmeijer, "Noninvasive Detection of Metastases and Follicle Density in Ovarian Tissue Using Full-Field Optical Coherence Tomography," Clin. Cancer Res, clincanres-0288 (2016).
17. F. Davnall, C. S. P. Yip, G. Ljungqvist, M. Selmi, F. Ng, B. Sanghera, B. Ganeshan, K. A. Miles, G. J. Cook, and V. Goh, "Assessment of tumor heterogeneity: an emerging imaging tool for clinical practice?" Insights Imaging **3**(6), 573–589 (2012).
18. G. Castellano, L. Bonilha, L. M. Li, and F. Cendes, "Texture analysis of medical images," Clin. Radiol. **59**(12), 1061–1069 (2004).
19. D. R. Chen, R. F. Chang, and Y. L. Huang, "Computer-aided diagnosis applied to US of solid breast nodules by using neural networks," Radiology **213**(2), 407–412 (1999).
20. K. Holli, A. L. Lääperi, L. Harrison, T. Luukkaala, T. Toivonen, P. Ryymin, P. Dastidar, S. Soimakallio, and H. Eskola, "Characterization of breast cancer types by texture analysis of magnetic resonance images," Acad. Radiol. **17**(2), 135–141 (2010).
21. S. Nandy, A. Mostafa, P. D. Kumavor, M. Sanders, M. Brewer, and Q. Zhu, "Characterizing optical properties and spatial heterogeneity of human ovarian tissue using spatial frequency domain imaging," J. Biomed. Opt. **21**(10), 101402 (2016).
22. M. Tuceryan and A. K. Jain, "Texture analysis. In: Chen CH, Pau LF, Wang PSP, editors. The Handbook of Pattern Recognition and Computer Vision," World Scientific Publishing Co., pp. 207–248 (1998).
23. R. Lopes, A. Ayache, N. Makni, P. Puech, A. Villers, S. Mordon, and N. Betrouni, "Prostate cancer characterization on MR images using fractal features," Med. Phys. **38**(1), 83–95 (2011).
24. R. A. Brown and R. Frayne, "A comparison of texture quantification techniques based on the Fourier and S transforms," Med. Phys. **35**(11), 4998–5008 (2008).
25. K. W. Gossage, T. S. Tkaczyk, J. J. Rodriguez, and J. K. Barton, "Texture analysis of optical coherence tomography images: feasibility for tissue classification," J. Biomed. Opt. **8**(3), 570–575 (2003).
26. K. W. Gossage, C. M. Smith, E. M. Kanter, L. P. Hariri, A. L. Stone, J. J. Rodriguez, S. K. Williams, and J. K. Barton, "Texture analysis of speckle in optical coherence tomography images of tissue phantoms," Phys. Med. Biol. **51**(6), 1563–1575 (2006).
27. U. Alqasemi, P. Kumavor, A. Aguirre, and Q. Zhu, "Recognition algorithm for assisting ovarian cancer diagnosis from coregistered ultrasound and photoacoustic images: ex vivo study," J. Biomed. Opt. **17**(12), 126003 (2012).
28. A. Ly, A. Buck, B. Balluff, N. Sun, K. Gorzolka, A. Feuchtinger, K. P. Janssen, P. J. Kuppen, C. J. van de Velde, G. Weirich, F. Erlmeier, R. Langer, M. Aubele, H. Zitzelsberger, L. McDonnell, M. Aichler, and A. Walch, "High-mass-resolution MALDI mass spectrometry imaging of metabolites from formalin-fixed paraffin-embedded tissue," Nat. Protoc. **11**(8), 1428–1443 (2016).

1. Introduction

Ovarian cancer is the fifth leading cause of cancer death among women and has the lowest survival rate among all the gynecological cancers [1]. This is mainly due to the late stage detection (stage III and IV), which in turn can be attributed to the lack of effective early screening and diagnostic techniques. Standard preventive procedure for high-risk women includes prophylactic oophorectomy (PO) [2]. However, the mortality rate of women undergoing premenopausal oophorectomy seems to increase considerably [3]. As a result, it is extremely necessary to develop sensitive tools for detection of early stage ovarian cancers. Almost 95% of the ovarian cancers occur in the epithelial layer surrounding the ovarian tissue. Imaging modalities e.g. photoacoustic tomography (PAT), photoacoustic microscopy (PAM), confocal microendoscopy have previously been applied for diagnosis of ovarian cancer [4–6], however H&E based histology still remains the gold standard for clinical diagnosis.

Optical coherence tomography (OCT) has proved to be useful for *ex vivo* and *in vivo* detection of ovarian cancer, mainly because it can detect the microscopic changes in the stromal collagen distribution which results in alteration of tissue scattering and elasticity [7–9]. In general, point detectors or line detectors are required for generating OCT images. However, this requires extensive scanning, and is limited by the field of view. Full field optical coherence tomography (FFOCT) which is an extension of conventional OCT, can

Biomedical Optics EXPRESS

acquire high resolution *en face* interferometric images with an area detector e.g. a CMOS or CCD camera. The axial resolution is determined by the bandwidth of the light source, which is generally a very broadband low cost halogen lamp. This can provide a very high axial resolution of 1-2 μm, compared to the conventional SLD based sources [10,11]. The transverse resolution of the system can be controlled by the numerical aperture of the microscope objectives and the source wavelength. FFOCT provides greater contrast and depth of penetration compared to confocal microscopy [12]. FFOCT has been used for diagnosis of fixed and non-fixed tissue samples for the detection of breast, lung and skin and ovarian tissues [13–16].

Morphological heterogeneity of tumor tissue has recently emerged as an important diagnostic parameter [17, 18]. Morphological analysis, which involves detecting changes in the gray level intensity of a medical image, has been successfully used for differentiating between normal and malignant pathologies using several imaging modalities, such as Ultrasound, MRI and Spatial frequency domain imaging [19–21]. Several approaches of texture analysis have been demonstrated. These include statistical methods such as histogram analysis, mathematical model based approach including fractal analysis as well as transform based methods including Wavelet, Fourier and Gabor transform [22–24]. Conventional OCT has also been applied for texture analysis of tissues [25,26]. However, the resolution of all the imaging modalities explored is difficult to compare with high resolution H&E stained images. Histology, which can provide microscopic tissue information with high degree of accuracy, is currently limited by staining methods and long staining time. FFOCT on the other hand can provide rapid high resolution, label-free images of tissue with comparable accuracy. So far, most of the studies on FFOCT have relied on visual observation of normal and malignant structures. This limits the interpretation across different observers, and may affect the ultimate diagnosis. Automated image analysis methods can provide a robust and accurate diagnosis independent of visual interpretation limitations. In this paper, we have explored the feasibility of using a FFOCT system for imaging and analysis of human ovarian tissue samples. Five features were quantitatively extracted from normalized histogram of the normal and malignant FFOCT images. These were the mean, standard deviation, skewness, kurtosis and entropy. The sensitivity, specificity as well as the area under the receiver operating characteristic (ROC) curve (AUC) was evaluated for diagnostic accuracy. To the best of our knowledge, this is the first ever study to report the quantitative morphological analysis and feature extraction using FFOCT for classification of normal and malignant human ovarian tissue. Quantitative information from FFOCT images can be invaluable for high resolution, label free, rapid *ex vivo* diagnosis of neoplastic changes related to ovarian cancer.

2. Materials and methods

2.1 Ovary sample

De-identified formalin fixed paraffin embedded (FFPE) tissue blocks of human ovarian tissue samples were acquired from University of Massachusetts (UMass) Memorial Cancer Center and University of Connecticut Health Center (UCHC). After imaging, the slides corresponding to the imaged planes were identified, and stained using hematoxylin and eosin (H&E) for diagnosis.

2.2 FFOCT system

Figure 1(a) shows the configuration of the FFOCT system, which is based on a Linnik interferometer consisting of two objective lenses (10X, N.A. 0.25), one each in the reference and sample arm. A 6 V, 20 W halogen lamp (central wavelength 560 nm, bandwidth 200 nm) customized with Köhler illumination was used to illuminate the sample. The reference mirror was connected to a piezo stage (Thorlabs, NF5DP20) and the samples were placed on a 3D stage. The *en face* interferometric images were captured by a 12 bit CCD camera (Basler

Biomedical Optics EXPRESS

acA1300-30um, 1296 x 966 pixels, 30 fps). The axial resolution of the system was measured from the FWHM of the axial PSF to be 1.6 μm as shown in Fig. 1(b). The lateral resolution was measured by calculating the PSF from the derivative of the edge spread function (ESF) of a sharp blade and was around 3.9 μm, shown in Fig. 1(c).

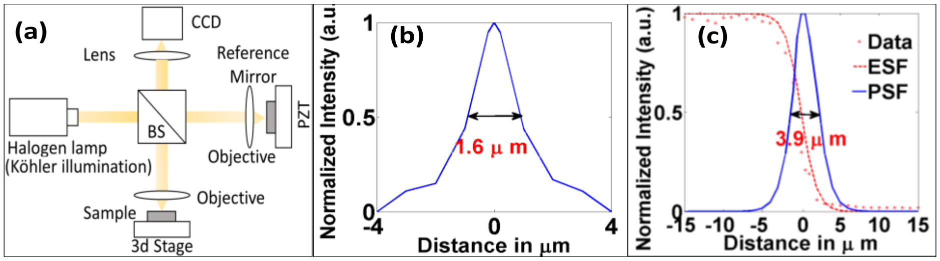

Fig. 1. (a) FFOCT setup; (b) Axial resolution; (c) Lateral resolution

2.3 FFOCT imaging procedure

FFPE ovarian tissue blocks were placed on a 3D stage and four phase shifted *en face* images were acquired with the CCD camera, from which the OCT image was computed. The field of view was 0.8 cm x 0.8 cm. The depth of penetration was around 100 μm. Overall acquisition time for each location was 0.3 seconds. The OCT images were then compared with the H&E slides by our pathologist for identification of benign and malignant ovarian tissue features.

2.4 Feature extraction

Each image (0.8 cm x 0.8 cm) was further divided into several non-overlapping sub-images (0.15 cm x 0.15 cm), based on the pathologist's observation of normal and malignant structures. Five features were extracted quantitatively using MATLAB from the analysis of the normalized histogram of these normal and malignant FFOCT ovary images. If x is the i^{th} pixel gray level and N is the total number of pixels, then the five features can be computed from Eqs. (1) to (5).

$$\text{Mean } (\mu) = \frac{1}{N}\sum_{i=1}^{N} x_i \tag{1}$$

$$\text{Variance } (\sigma^2) = \frac{1}{N}\sum_{i=1}^{N} (x_i - \mu)^2 \tag{2}$$

$$\text{Skewness} = \frac{1}{N}\sum_{i=1}^{N}\left[\frac{(x_i-\mu)}{\sigma}\right]^3 \quad (3) \quad \text{Kurtosis} = \frac{1}{N}\sum_{i=1}^{N}\left[\frac{(x_i-\mu)}{\sigma}\right]^4 - 3 \tag{4}$$

$$\text{Entropy} = -\sum_{i=1}^{N} p(x_i)\log_2 p(x_i) \tag{5}$$

Mean was used to measure the average pixel intensity. The deviation of the histogram distribution was calculated from the variance. Kurtosis and skewness signified the flatness and asymmetry of the image histogram. Entropy was used to signify the irregularity of the image. It was assumed that identification of one image from a sample as cancer was sufficient to classify the ovary as malignant, and only if every image from a sample was found to be normal then the ovary was considered normal [27]. In general, lower mean value of an image combined with higher values of variance, entropy, skewness and kurtosis signified increased heterogeneity of the image, which can be associated with development and progression of cancer. A logistic regression model was used to classify the normal and malignant ovarian tissue groups. The five features extracted from FFOCT images were used as predictor variables, and response variable was the actual diagnostic results (1 representing malignant

Biomedical Optics EXPRESS

and 0 representing normal). The coefficients of the linear model were determined by MATLAB GLMFIT function and then the same set of coefficients were applied to MATLAB GLMVAL function to calculate the responses of the testing set. The quality of the model was evaluated using ROC curve and AUC.

3. Results and discussions

A total of 14 ovarian tissue samples were imaged *ex vivo* with the FFOCT system, consisting of 7 benign and 7 malignant samples. The malignant tissue samples consisted of 4 cases of serous carcinoma, 2 cases of mucinous carcinoma and 1 endometroid carcinoma. Figure 2 shows the FFOCT images of a normal and malignant ovarian tissue (serous carcinoma) along with the corresponding H&E stained histology images. It can be observed from the FFOCT and histology images that normal ovarian tissue has visibly smoother and homogeneous stroma with dense collagen distribution, while the malignant ovary has highly degenerated, fragmented and heterogeneous stroma, characterized by poorly differentiated and clustered tumor architecture.

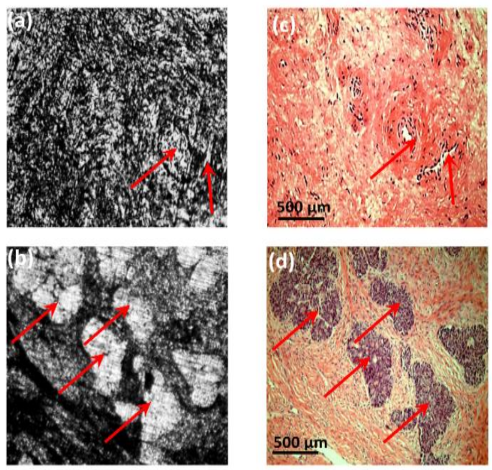

Fig. 2. FFOCT images of (a) normal and (b) malignant ovary; corresponding histology images are shown in (c,d). The matching areas are indicated by red arrows.

Five features were extracted from normalized histogram of 56 non-overlapping FFOCT images (28 normal and 28 malignant). Figure 3 shows the boxplot and p values of the features normalized mean, variance, kurtosis, skewness and entropy. It can be observed from Fig. 3 that the malignant tissue group has lower mean intensity value compared to the normal group, which may be attributed to aggravated necrosis and reduced collagen concentration. Additionally, the variance, kurtosis, skewness and entropy of the malignant group were significantly higher, signifying more heterogeneity and clustering associated with development of cancer.

For classification between normal and malignant ovarian tissue groups, the images were separated into two groups, 36 images were used for training (18 normal, 18 malignant) the logistic classifier and 20 images (10 normal, 10 malignant) were tested using the logistic regression model. Figure 4 shows the ROC curves for both the training and testing sets. For the training set, a sensitivity and specificity of 95.3% and 91.1% was obtained, with average AUC at 95% confidence interval being 0.93, while for the testing set, we obtained a sensitivity of 91.6% and specificity of 87.7%, with average AUC of 0.89 at 95% confidence interval.

The current work has several limitations. The training and testing results are based on a limited sample pool, and more data needs to be acquired for further validation. Additionally, only FFPE tissue blocks were used for this preliminary study. Although, some previous spectroscopic imaging studies have indicated that classification of fresh and FFPE tissues produce comparable results [28], however, further compatibility studies need to be conducted between these two tissue groups. Menopausal status of the patients, which was not available for the samples studied, also needs to be considered for more accurate analysis. Also, a lower NA objective lens was used, and much higher cellular level transverse resolution can be obtained by using high NA objective lenses, as shown by other FFOCT studies. The current study is intended to be implemented as a rapid *ex vivo* alternative for conventional H&E based histology, which requires staining and long diagnostic waiting time. The intended use is taking a biopsy sample and performing rapid optical diagnosis of normal and malignant tissues based on FFOCT images, which are comparable in resolution to standard histology methods and do not require staining. Future work will include studying freshly excised tissue samples and incorporating the data processing and feature extraction methods in real time, so that the technology can be translated from bench to bedside.

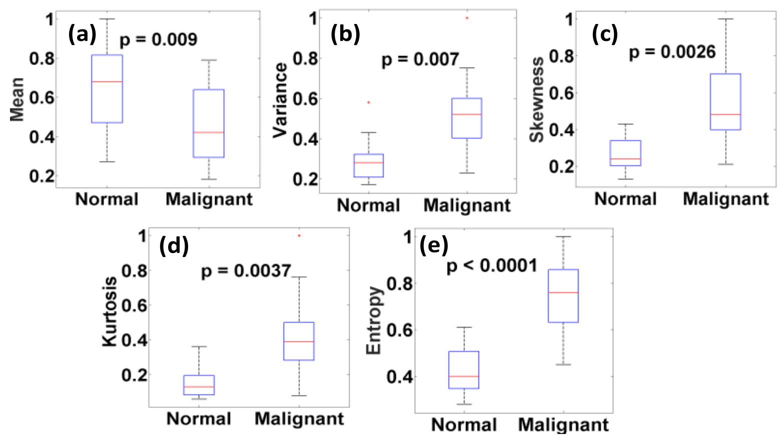

Fig. 3. Boxplot of the five features with p values for (a) mean, (b) variance, (c) skewness, (d) kurtosis and (e) entropy.

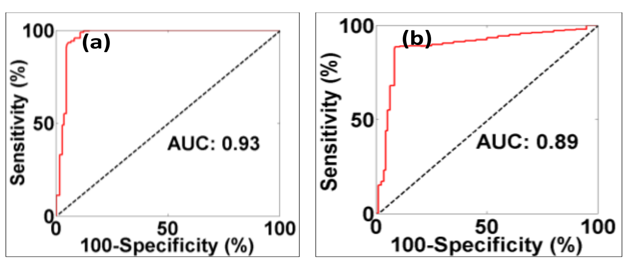

Fig. 4. ROC curve for training and testing using the five features.

4. Summary

In this study, 14 human ovarian tissue samples were imaged *ex vivo* using the FFOCT system, and five quantitative features were extracted from the normal and malignant ovarian tissue images. Using a logistic classifier model, a sensitivity of 91.6% and specificity of 87.7% was achieved. The initial promising results indicate that FFOCT can potentially be a very useful *ex vivo* diagnostic tool for label free, rapid and low cost quantitative analysis of ovarian tissue, and reduce the waiting time associated with the conventional histology.

Funding

This study was supported by National Institute of Health (R01CA151570).